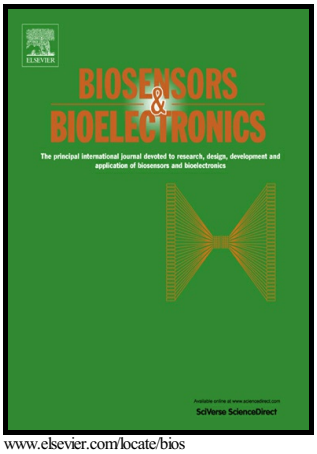

www.elsevier.com/locate/bios

Ultra-miniaturization of a planar amperometric sensor targeting continuous intradermal glucose monitoring

Federico Ribet, Göran Stemme, Niclas Roxhed

PII: S0956-5663(16)30999-X
DOI: http://dx.doi.org/10.1016/j.bios.2016.10.007
Reference: BIOS9228

To appear in: *Biosensors and Bioelectronic*

Received date: 13 July 2016
Revised date: 23 September 2016
Accepted date: 3 October 2016

Cite this article as: Federico Ribet, Göran Stemme and Niclas Roxhed, Ultra miniaturization of a planar amperometric sensor targeting continuous intraderma glucose monitoring, *Biosensors and Bioelectronic* http://dx.doi.org/10.1016/j.bios.2016.10.007

Ultra-miniaturization of a planar amperometric sensor targeting continuous intradermal glucose monitoring

Federico Ribet*, Göran Stemme, Niclas Roxhed

Department of Micro and Nanosystems, KTH Royal Institute of Technology, Stockholm, 100 44, Sweden

*Corresponding author. tel.: +46 73 7652 382; ribet@kth.se.

Abstract

An ultra-miniaturized electrochemical biosensor for continuous glucose monitoring (CGM) is presented. The aim of this work is to demonstrate the possibility of an overall reduction in sensor size to allow minimally invasive glucose monitoring in the interstitial fluid in the dermal region, in contrast to larger state-of-the-art systems, which are necessarily placed in the subcutaneous layer. Moreover, the reduction in size might be a key factor to improve the stability and reliability of transdermal sensors, due to the reduction of the detrimental foreign body reaction and of consequent potential failures. These advantages are combined with lower invasiveness and discomfort for patients. The realized device consists of a microfabricated three-electrode enzymatic sensor with a total surface area of the sensing portion of less than 0.04 mm^2, making it the smallest fully integrated planar amperometric glucose sensor area reported to date. The working electrode and counter electrode consist of platinum and are functionalized by drop casting of three polymeric membranes. The on-chip iridium oxide (IrOx) pseudo-reference electrode provides the required stability for measurements under physiological conditions. The device is able to dynamically and linearly measure glucose concentrations in-vitro over the relevant physiological range, while showing sufficient selectivity to known interfering species present in the interstitial fluid, with resolution and sensitivity (1.51 nA/mM) comparable to that of state-of-art commercial CGM systems. This work can therefore enable less invasive and improved CGM in patients affected by diabetes.

Keywords: Glucose biosensor; MEMS; Diabetes; Continuous glucose monitoring; Amperometry; Iridium oxide reference electrode.

1. Introduction

Diabetes mellitus (DM) is a set of metabolic disorders caused by either a faulty bodily response (T2DM) or an underproduction in the pancreas (T1DM) of insulin, which regulates the metabolism of carbohydrates and controls hyperglycemia. These diseases lead to unstable and dangerously high oscillations of the glucose level in the body (Vaddiraju et al., 2010a). According to the International Diabetes Federation, diabetes is now affecting 387 million people, and was responsible for 4.9 million deaths worldwide in 2014. Although diabetes is not curable, proper diabetes management is essential to avoid numerous possible complications, both on a short and a long term, such as hypoglycemia, cardiovascular diseases, neuropathy, retinal damage, nephropathy and amputations (Bailes, 2002). Traditionally, patients perform self-monitoring of their glycaemia through capillary blood sampling by finger pricking. Even though the measurement results are very reliable, there are several drawbacks for the patient, such as pain, risk of infections, lesions, and sensory loss, combined with an incomplete temporal picture resulting from 4-5 daily data points (Le Floch et al., 2008). To limit risks and improve the treatment, research in the field of real-time glucose monitoring of interstitial fluid (IF) has gained much attention in the last two decades. In fact, continuous glucose monitoring (CGM) can significantly enhance the quality of the treatment, offering a

complete picture of glycaemia evolution, while dramatically reducing the discomfort of regular finger pricks required by conventional methods (The Diabetes Control and Complications Trial Research Group, 1993).

To monitor glycaemia, electrochemical enzymatic glucose sensing currently remains the most reliable monitoring technique available (Heller and Feldman, 2008; Vashist et al., 2011; Wang, 2008). Several alternatives have been investigated (Ferrante do Amaral and Wolf, 2008; Gifford, 2013; Vashist, 2012), including enzyme-free detection principles (Chen et al., 2013, 2014; Park et al., 2006; Toghill and Compton, 2010), without being able to supplant the former standard enzymatic principle.

Implantable sensors have been studied and used in a broad range of medical applications (Pang et al., 2013; Receveur et al., 2007), such as pressure sensing (Clausen and Glott, 2014; Yu et al., 2014), neural and muscular monitoring (Gosselin, 2011; Shivashankar et al., 2014), as well as biosensing (Frost and Meyerhoff, 2002; Li et al., 2007; Vaddiraju et al., 2010b) and CGM (Hovorka, 2006).

Implantable continuous glucose monitoring systems based on electrochemical sensing have been available on the market for over a decade (e.g. products by Medtronic, Dexcom, and Abbott). These products consist of flexible strips implanted in the hypodermis, measuring the glucose concentration in the IF. However, although more convenient than traditional devices, these products are not as reliable as blood measurements and cannot yet be considered neither non-invasive nor painless due to their large needle-based insertion mechanism. For example, the most recent product on the market consists of a sensor strip of 5 x 0.6 mm^2 (Csöregi et al., 1995; Feldman et al., 2003; Heller and Feldman, 2010), inserted under the skin through a 6 mm long half-pipe hypodermic needle. Other smaller planar amperometric glucose sensors have been previously published (Li et al., 2009; Weltin et al., 2014a; Yang et al., 2004), but all with a total sensing portion exceeding 0.4 mm^2 and with a length in the insertion direction greater than 3 mm.

The aim of this work is to investigate the possibility of a further significant sensor miniaturization, not only to permit reduction of the invasiveness and the discomfort related to current CGM systems, but especially to enable directly access the interstitial fluid of the dermal region in the skin (Fig. 1). In particular, the objective is to realize a complete microfabricated sensor with electrodes geometrically arranged to potentially fit on a probe with a length in the insertion direction significantly shorter than 1 mm, which represents the average depth of human forearm dermis (Hwang et al., 2016), and narrower than 75 µm for the ease of insertion (Davis et al., 2004). In fact, it has been shown that optimal access to IF is achieved in the dermal region. In this location IF is more abundant than in the underlying subcutaneous tissue, in which, in addition, the inhomogeneity of the adipose tissue and the size of the adipocytes may also detrimentally affect the IF solutes' concentration (Cengiz and Tamborlane, 2009). Feasibility of glycaemia monitoring in the dermal interstitial fluid has been previously demonstrated by IF extraction (Bantle and Thomas, 1997; El-Laboudi et al., 2013; Hilgers et al., 2001; Mukerjee et al., 2004; Wang et al., 2005). Moreover, there are indications that glucose concentration in the dermal IF best matches the amplitude and dynamics of blood and plasma glucose (Groenendaal et al., 2008). Finally, the implant size plays a role in the extent of the foreign body reaction (FBR), which is detrimental for in-vivo measurements. In fact, the FBR increases proportionally to the initial tissue trauma during insertion, which relates to the degree of acute inflammation, and to the implant size, which is responsible for the development of the fibrous capsule (Burgess et al., 2015).

In this paper we describe a planar amperometric glucose sensor with the smallest electrode footprint area reported up to date, which, despite the decreased size (overall area of the sensing portion of less than 0.04 mm^2) and the related challenges, is able to selectively measure physiologically relevant glucose concentrations in-vitro, with a resolution and a sensitivity comparable to commercial CGM systems.

2. Materials and methods

2.1. Working principle

The amperometric sensor is based on the selective transformation of glucose molecules through glucose oxidase (GOx) into hydrogen peroxide (H_2O_2). The concentration of H_2O_2 is then anodically detected at the surface of the working electrode (WE), when a bias of +0.6 V is applied, according to the following set of reactions (Heller and Feldman, 2008; Li et al., 2009):

$$\text{Glucose} + O_2 \xrightarrow{\text{GOx}} \text{Gluconic acid} + H_2O_2 \quad (1),$$

$$H_2O_2 \xrightarrow{+500\ \text{mV vs. IrOx}} O_2 + 2H^+ + 2e^- \quad (2),$$

while at the counter electrode (CE) the current flow is balanced by the reduction reaction:

$$2H^+ + \tfrac{1}{2}\, O_2 + 2e^- \rightarrow H_2O \quad (3).$$

Since oxygen is involved in reaction *(1)*, an excess of O_2 with respect to glucose must be ensured at the WE surface in order to avoid undesirable saturation effects in the physiologically relevant glucose range. Moreover, at +0.6 V, other electroactive substances commonly present in the IF, such as uric acid and ascorbic acid, interfere with the detection of hydrogen peroxide, being undesirably oxidized, and contribute to the overall current, thus generating a false glucose reading. As a consequence, additional precautions are needed at the WE to ensure correct operation and selectivity of the sensor. Finally, in order to keep the WE potential fixed (and hence for the sensor to be stable and provide a reliable response over time) a third electrode, acting as reference, is necessary (Waleed Shinwari et al., 2010).

2.1.1 Pseudo-reference electrode

When miniaturizing electrochemical components, the traditional macroscopic reference electrode configuration cannot be realized and a pseudo-reference electrode (Q-RE) must be used. Integrating a reliable Q-RE represents a key challenge for microsensors. The standard material historically used as a reference electrode in these applications is silver-silver chloride (Ag/AgCl). Its use for microprobes has been shown through chlorination of thick electrodeposited silver layers (Suzuki et al., 1998; Weltin et al., 2014b) and Cl-plasma treatment (Park et al., 2003). Despite the well-known behavior of Ag/AgCl, when these electrodes are microfabricated they typically have a very short lifetime due to dissolution of the thin AgCl layer, and when the chloride coating is dissolved the standard potential radically changes (Yang et al., 2004). This behavior, in combination with concerns about toxicity of the AgCl solute and the related inflammatory response, makes Ag/AgCl a less than optimal candidate for long-term in-vivo measurements, especially in ultra-miniaturized devices. A promising alternative to overcome the described limitations is the use of an iridium oxide (IrOx) electrode, which has been previously demonstrated to be a good candidate for miniaturized pseudo-reference electrodes for in-vivo applications (Tolosa et al., 2013; Yang et al., 2004). In fact, IrOx shows good biocompatibility, mechanical stability and minimal potential drift. Despite its strong open circuit potential dependence on the pH of the solution (- 77 mV/pH), IrOx is a reliable enough reference electrode in specific environments such as buffered solutions or interstitial fluid, where the pH variations are small and regulated in the range between 6.8 and 7.4 (Marunaka, 2015). Furthermore, it shows minimal long-term potential drift, and allows for the use of thin films (sub-100 nm thickness) deposited by standard microfabrication technologies, followed by a simple one-step activation procedure in a phosphate buffered saline (PBS) solution. Finally, with respect to Ag/AgCl, IrOx shows much lower sensitivity to electroactive species present in the IF (Bezbaruah and Zhang, 2002; Marzouk et al., 1998).

2.2. Electrode design

The presented sensor consists of a standard three-electrode configuration including a working electrode and a counter electrode made of platinum, and an on-chip integrated pseudo-reference electrode made of oxidized iridium. In this design, each of the three electrodes has a surface area of 0.012 mm^2 (170 x 70 μm^2), with an inter-electrode distance of 10 µm, in order to maximize the active surface on the desired total sensor area and, at the same time, minimize ohmic losses. The resulting total sensing portion footprint is 0.037 mm^2 (530 x 70 μm^2).

While there are clear medical advantages, as described in the introduction, the miniaturization of this kind of sensors intrinsically entails challenges in signal amplitude, stability, choice of the active materials and valid fabrication processes. In fact, the amperometric current generated in the sensor is in a first approximation proportional to the active surface of the working electrode, and the reference electrode stability is decreased with the size reduction as well (Janata, 2009). Only the noise level, the electrode polarization and the ohmic losses are expected to be lowered and favor the performance when shrinking the device and placing the three electrodes on the same substrate. Despite the low currents involved in an amperometric sensor of this size, a three electrode setup has been chosen to guarantee better stability of the IrOx electrode

even at high glucose concentrations. A significant drift in the current response at glucose concentrations above 200 mg/dL was previously reported in the case of a basic two-electrode configuration (Tolosa et al., 2013).

2.3. Chemicals and instrumentation

Phosphate buffered saline (PBS, pH 7.4), glucose oxidase (Aspergillus niger, type VII), bovine serum albumin (BSA), glutaraldehyde grade I (GA, 25%), d-(+)-glucose, Nafion® 117 (5 wt% solution in a mixture of lower aliphatic alcohol and water), polyurethane Selectophore™ (PU), tetrahydrofuran (THF), N,N-dimethylformamide (DMF), L-ascorbic acid (AA) and uric acid (UA) were purchased from Sigma-Aldrich and used as received, if not specified otherwise.

The quality of the deposited materials and of the polymeric membranes have been controlled through scanning electron microscopy (SEM) and optical microscopy respectively, while the thickness of the membranes has been measured using a mechanical profiler. Electrochemical measurements were performed using a sub-picoampere resolution potentiostat (DY2011, Digi-Ivy, Inc.). A commercial 3M Ag/AgCl reference electrode (REF321, Radiometer Analytical) was used as a reference during electrode preparation. All potentials are referred to a saturated Ag/AgCl reference electrode, if not specified otherwise. For simplicity and to limit evaporation of the testing solutions during long term characterization, all experiments were performed at 26 °C, unless stated otherwise.

2.4. Device fabrication

2.4.1 Wafer level processing

The microsensors have been produced using standard photolithography and microfabrication technologies on a 100 mm <100> silicon substrate and have been processed as follows. A 1-µm thick silicon dioxide layer was thermally grown on the Si wafer to electrically insulate the electrodes from the substrate. 150 nm of platinum were deposited using electron-beam evaporation over a 20 nm chromium adhesion layer and patterned via lift-off in order to define electrodes, contacts and interconnections on the different chips. A 200 nm silicon nitride (Si_3N_4) layer was then deposited using plasma enhanced chemical vapor deposition (PECVD). Openings, corresponding to contact pads and active sites of the microelectrodes, were defined using photolithography and wet etched in a buffered hydrofluoric acid 7:1 aqueous solution. Finally, 80 nm of iridium was selectively deposited using electron-beam evaporation on top of only the Q-RE microelectrode sites, over a 20 nm thick titanium adhesion layer, through a second lift-off step. The fabrication process is illustrated in Fig. 2.

2.4.2 Electrode functionalization

To obtain the desired IrOx layer on top of the evaporated iridium at the Q-RE site, cyclic voltammetry was used. It is known that cycling the potential of iridium between oxygen and hydrogen evolution extremes leads to the creation of a thin oxide layer on the surface (Juodkazyte et al., 2005; Li et al., 2009). The process was carried out in a 0.1 M PBS solution, pre-deaerated for 10 minutes by nitrogen bubbling. The potential of the electrode was then cycled 30 times between the extremes -0.75 V and +0.95 V, with a sweep rate of 200 mV/s, using a separate platinum strip as counter electrode and the Ag/AgCl electrode as reference.

Subsequently, three additional membranes were deposited on the sensing region, in order to guarantee the desired performances in term of specificity, linearity and selectivity, respectively. All the membranes were placed by drop casting and were allowed to dry for 45 min each before further processing. The first layer, which embeds the enzyme and is responsible for the H_2O_2 generation from glucose molecules, was deposited using two aqueous solutions, consisting of 100 nL of 3 wt% GOx and 3 wt% BSA, and 100 nL of 2 wt% glutaraldehyde respectively, with the latter acting as a crosslinker. The second layer consists of a permselective membrane, made from 800 nL of 3 wt% PU in a solution of 97% THF and 3% DMF. Due to the different diffusivity of glucose and oxygen through the PU layer, the linear range can been extended to guarantee sufficient resolution over the entire physiological glucose concentration range and avoid saturation (Koudelka et al., 1989). The third semipermeable layer was made from a solution of 5 wt% Nafion and is used to exclude anionic electroactive substrates, such as UA and AA, present in the IF (Fan and Harrison, 1992; Tolosa et al., 2013). Nafion coatings have previously been shown to be permeable and allow transport of cations and neutral species, as well as supporting electrolytes, while rejecting negatively

charged substrates (Harrison et al., 1988; Turner et al., 1990). In addition to the increase in selectivity, this layer protects the reference electrode from fouling and, hence, increases the stability of the sensor over time (Li et al., 2009). Additionally, Nafion encapsulation has shown a good degree of biocompatibility, and is therefore a suitable interface for long term implantation use (Turner et al., 1991). After preparation, the sensors were stored dry and thoroughly washed with DI water before being used for measurements.

3. Results and discussion

Fig. 3(A) shows an optical image of the top of the complete chip, after membrane casting. For the ease of manipulation and in-vitro testing, the contact portion of the chip has been kept macroscopic (around 1 cm^2 overall), while the targeted miniaturization of the active region of the sensor has been successfully attained. A reduction in total surface of the sensing portion of more than nine-fold has been achieved with respect to previous work (Yang et al., 2004) and a nearly forty-fold decrease has been obtained if compared to state-of-the-art products, e.g. Abbott's Freestyle™ systems (Feldman et al., 2003). The latter commercial sensor, together with its insertion needle, is shown in Fig. 3(B) in comparison to our bare microfabricated sensor. The developed sensor, with a total sensing portion footprint of 530 x 70 μm^2, is small enough to potentially allow direct continuous glucose monitoring in the dermal region. The small size may also improve the durability and reliability of transdermal sensors themselves, due to the consequent limitation of detrimental FBR effects caused by their insertion and prolonged implantation. These advantages are combined with the fact that such a miniaturized device can result in virtually painless insertion into the skin, since its small size reduces the risk of encountering or stimulating a nerve, and hence of producing a painful sensation (Prausnitz, 2004).

3.1. Pseudo-reference electrode stability

A fundamental requirement for the on-chip integrated Q-RE is to maintain, under standard physiological conditions, a constant potential over time to provide a stable reference to the system. To assess the stability of the IrOx electrode, the open circuit potential (OCP) of fabricated iridium oxide pseudo-reference electrodes was measured in PBS, using a platinum strip as the CE and the Ag/AgCl electrode as a reference. Long term stability of the open circuit potential of the produced Q-RE was evaluated over a four-day period, and a typical OCP curve is shown in Fig. 4. The inset in Fig. 4 shows the short term OCP of the Q-RE used in the ensuing measurements, immediately after oxidation in a deaerated PBS solution.

The obtained results partially differ from earlier reported behavior (Yang et al., 2004). In that study, a radical change of the OCP was measured after 24 hours, due to hydration of the IrOx film (Yao et al., 2001), after which a stable plateau was reached and maintained for the following nine days. In our study the OCP of the IrOx electrodes never changed significantly over a four-day time frame. A probable explanation of the different behavior seen in this study with respect to earlier results (Yang et al., 2004) is the different technique used for the deposition of the iridium layer and its oxidation, namely e-beam evaporation and successive electrochemical oxidation in our case, instead of direct IrOx electrodeposition. Nevertheless, the standard deviation is comparable (around ± 10 mV), combined with a negligible drift over time in both cases. If the inter-electrode OCP variation is smaller than few tens of mV, it is then sufficient to properly choose the applied bias voltage, i.e. a voltage sufficient to always guarantee H_2O_2 oxidation without activating other unwanted reactions, in order to always guarantee correct functioning of the sensor. As an alternative for improved accuracy, sensor calibration can be performed, as currently required by several

commercial CGMS. The different absolute values of OCP shown in Fig. 4, 170 mV and 295 mV respectively, can be partially explained by a previously reported study (Juodkazyte et al., 2005), where IrOx electrodes showed different standard potential in deaerated and oxygen-containing solutions. In this work, the short term OCP measurements were performed immediately after CV in a previously N_2-bubbled PBS solution, while the long term OCP studies (inset in Fig. 4) were performed in freshly made PBS solutions. However, further investigation is needed to better understand the iridium oxidation process and to characterize, and possibly optimize, the thickness of the created oxide layer, which influences the long-term stability. Additionally, the oxidation of iridium can occur in different states, depending on the activation conditions, such as oxidizing solution and CV parameters (Franklin et al., 2005; Juodkazyte et al., 2005; Yang et al., 2004). This influence on the OCP and the electrode stability have not been investigated in this work, even though a better understanding might improve durability and reproducibility of the produced electrodes.

3.2. Amperometric sensor response

Plot 5(A) reports the amperometric glucose detection as a function of time, as well as the response to interferents (UA and AA) of the sensor. The sensing portion of the chip was immersed in the measurement solution, consisting of magnetically stirred 0.1 M PBS, and allowed to stabilize for a few minutes, before applying a bias of +0.5 V to the WE with respect to the integrated Q-RE. When the background current reached a stable value, first uric acid and then ascorbic acid were added to the solution (with a final concentration of 100µM each) in order to test the selectivity of the sensor. Afterwards, aliquots of concentrated glucose solution have been regularly added to raise the overall glucose concentration from 0 to 500 mg/dL, in steps of 50 mg/dL. The entire measurement lasted for more than eight hours, in order to show the stability of the reference electrode over prolonged use and to simulate the intended application of the device. Plot 5(B) shows, for the same measurement, the current as a function of the glucose concentration and demonstrates excellent linearity up to 200 mg/dL and adequate resolution over the full range of interest.

The goal of this study was to investigate miniaturization beyond previously published devices, and it is interesting to note that the obtained sensing performances compare positively to both current commercial and research-level systems, although some of the earlier sensors have the clear advantage of having been tested in-vivo. The sensitivity of the sensor is 1.51 nA/mM in the linear range. In order for this values to be compared to larger electrodes from previous work, the sensitivity can also be normalized, dividing its value by the WE area, to 12.7 $\mu A \cdot mM^{-1} \cdot cm^{-2}$. The obtained sensitivity is directly comparable to 1.04 nA/mM (Feldman et al., 2003) and compares favorably, in terms of normalized sensitivity, to 0.7 $\mu A \cdot mM^{-1} \cdot cm^{-2}$ (Weltin et al., 2014a), 2.4 $\mu A \cdot mM^{-1} \cdot cm^{-2}$ (Yang et al., 2004), 2.5 $\mu A \cdot mM^{-1} \cdot cm^{-2}$ (Yang et al., 2002), 2 $\mu A \cdot mM^{-1} \cdot cm^{-2}$ (Koudelka et al., 1989), and 3.3 $\mu A \cdot mM^{-1} \cdot cm^{-2}$ (Vaddiraju et al., 2011).

Current International Organization for Standardization guidelines (ISO 15197:2013) require a resolution of ± 20% at glucose concentrations above 100 mg/dL, justified by the fact that an error up to 20% is very unlikely to lead to a wrong medical decision. In this regard, the noise would limit the measurement resolution to ± 5%; however, its influence can be completely eliminated by a simple averaging operation over time. Therefore, the main source of error, together with Q-RE drift, repeatability and reproducibility, is provided by the cross-sensitivity to endogenous interferents, which is hereafter analyzed in a worst-case scenario. At 26 °C, the sensor exhibits adequate rejection of electroactive interfering species: the effect on the measurement current is limited to 1.32 pA/µM for UA and 1.69 pA/µM for AA. Moreover, the selectivity and functionality of the sensor have been tested in a PBS solution at 34 °C, in order to better simulate the temperature in the dermal region (Liu et al., 2013), which is the targeted sensing location. This provides a more realistic characterization, since at higher temperature the reactivity of all involved species, including GOx (Li et al., 2009), increases. Aliquots of ascorbic acid, uric acid and glucose have been added to the solution at different increasing concentrations while recording the amperometric response. In particular, plot 5(C) shows a detailed response of the sensor to AA and UA at three different concentrations: low standard concentration (AA at 0.6 mg/dL, UA at 2 mg/dL), high standard concentration (also defined as therapeutic levels, AA at 0.9 mg/dL, UA at 5 mg/dL), and toxic concentration (AA at 2 mg/dL, UA at 10 mg/dL). The current generated by the lowest levels can be considered as a minimum fixed offset of 0.34 nA with respect to the background current, which in this case equals 0.045 nA. On the other hand, fluctuations at higher interferent concentrations must be considered as errors. At therapeutic levels, the maximum introduced error is lower than 2.5%, while the maximum effect on the current is 8.0% at high toxic concentrations, proving sufficient glucose selectivity even under extreme testing conditions.

Finally, the average response time, calculated between the instant of glucose addition and the time at which the current reaches 90% of the plateau value, is around 300 s, which corresponds to a reaction time of 10 $mg \cdot dl^{-1} \cdot min^{-1}$. The rate of glucose change in humans is typically lower than 3 $mg \cdot dl^{-1} \cdot min^{-1}$ (Dunn et al., 2004), and therefore the sensor would also manage to successfully track extreme glycaemia variations.

The linearity range, which is 0 to 200 mg/dL for the sensor shown, can be enhanced by simply increasing the thickness of the permselective PU layer, at the expense of the sensitivity; an increased thickness would provide a safer margin in case of hypoxemia, as previously shown (Feldman et al., 2003). In particular, an optimization of the trade-off between sensitivity and linearity should be performed, at a later stage when testing in-vivo, to balance performance and reliability under extreme medical conditions. While the described working principle has been verified on multiple sensors (n > 10), and has been tested also with different electrode sizes and geometries, the manual drop casting deposition inevitably results in membrane thickness variations. The average thickness of the three polymeric membranes and their variability were measured with a mechanical profiler. The results are reported in Table 1.

Table 1. Average thickness and thickness variability of the drop casting deposition process for the three different membranes (n = 6).

Deposited membranes	Thickness [µm]	Variation [µm]
Layer 1: GOx-BSA-GA	2.25	± 1
Layer 2: Polyurethane	19.5	± 4.5
Layer 3: Nafion	1	± 0.3

These variations were in fact found to directly affect the amperometric response parameters during characterization, in particular the sensitivity and the linearity range. For example, the variation in the polyurethane layer thickness from 15 to 24 µm results in a 60% reduction in sensitivity, as well as in an extended linear range. This can also be seen when comparing the response from the sensors in Fig 5(A) and 5(C) which were prepared using the same procedure. The second sensor has a higher sensitivity, which is partially due to the increased temperature (26 °C to 34 °C), but also due to a slightly thinner PU layer. On the other hand, this resulted in a reduced linearity range which is in accordance with the previously discussed trade-off between sensitivity and linearity. A proven and ideal solution to improve the reproducibility of the membrane deposition process would involve the use of more controllable and scalable membrane deposition techniques, e.g. automated CNC-based liquid dispensing (Weltin et al., 2014b) or inkjet printing (Wang et al., 2012). In fact, a typical inkjet drop is typical between 1-10 pL, which translates to a thickness resolution in the order of 100 nm for the previously mentioned materials. This would result in negligible inter-sensor membrane thickness variations and, hence, likely more reproducible results. Additionally, this would also allow the enzyme layer to be placed on top of only the working electrode, thereby improving sensor performance. Nevertheless, despite the non-ideal deposition conditions, the sensors fulfilled the initial requirements in terms of performance and overall size, and thus demonstrated the prospect of a significant possibility of down scaling for amperometric continuous glucose monitoring systems.

Further sensor miniaturization has also been investigated; for example, a microsensor having a sensing portion surface of 385 x 60 μm^2 and a thicker PU membrane guaranteeing excellent linearity up to glucose concentrations above 600 mg/dL has been realized and tested. At this size and conditions the signal is still clearly detectable; however, the sensitivity drops dramatically and reduces to 0.03 nA/mM (data not shown).

Future challenges for this work include integration of the described electrodes on mechanically resistant probes allowing in-vivo intradermal measurement of the glucose concentration in interstitial fluid. In this regard, additional precautions may be needed in order to guarantee proper functionality in presence of other exogenous interferents (e.g. acetaminophen), or in case of extreme hypoxemia, as previously discussed. Sufficient robustness (or protection) of the polymeric coatings has also to be provided for a safe insertion.

4. Conclusions

The smallest microfabricated amperometric glucose sensor area for applications in intradermal continuous glucose monitoring has been presented. The device has been demonstrated to dynamically and linearly measure physiologically

relevant glucose concentrations in-vitro, while showing sufficient selectivity to known electroactive species present in the interstitial fluid, with resolution and sensitivity comparable to that of commercial CGM systems and which satisfy ISO guidelines. The basic fabrication process is simple and robust, but further improvements can be reached by exploiting a more specific, precise and controlled membrane deposition technique on the three electrodes, to enhance performance, stability and reproducibility. With a total sensor area of less than 0.04 mm^2, the achieved miniaturization potentially allows CGM in dermal interstitial fluid. This work might therefore enable minimally invasive and enhanced glucose monitoring, and hence improve the quality of the treatment of patients affected by diabetes mellitus.

Acknowledgements

This work has been financially supported by Vinnova, via the Eurostars™ programme (joint initiative of EUREKA and the European Community), project no. E!8573.

References

Bailes, B.K., 2002. AORN J. 76, 266–282.

Bantle, J.P., Thomas, W., 1997. J. Lab. Clin. Med. 130, 436–441.

Bezbaruah, A.N., Zhang, T.C., 2002. Anal. Chem. 74, 5726–5733.

Burgess, D.J., Wang, Y., Vaddiraju, S., Gu, B., Papadimitrakopoulos, F., 2015. J. Diabetes Sci. Technol. 9, 966–977.

Cengiz, E., Tamborlane, W. V, 2009. Diabetes Technol. Ther. 11 Suppl. 1, S11–6.

Chen, C., Xie, Q., Yang, D., Xiao, H., Fu, Y., Tan, Y., Yao, S., 2013. RSC Adv. 3, 4473–4491.

Chen, X., Wu, G., Cai, Z., Oyama, M., Chen, X., 2014. Microchim. Acta 181, 689–705.

Clausen, I., Glott, T., 2014. Sensors 14(9), 17686-17702.

Csöregi, E., Schmidtke, D.W., Heller, a, 1995. Anal. Chem. 67, 1240–1244.

Davis, S.P., Landis, B.J., Adams, Z.H., Allen, M.G., Prausnitz, M.R., 2004. J. Biomech. 37, 1155–63.

Dunn, T.C., Eastman, R.C., Tamada, J.A., 2004. Diabetes Care 27, 2161–2165.

El-Laboudi, A., Oliver, N.S., Cass, A., Johnston, D., 2013. Diabetes Technol. Ther. 15, 101–15.

Fan, Z., Harrison, D.J., 1992. Anal. Chem. 64, 1304–1311.

Feldman, B., Brazg, R., Schwartz, S., Weinstein, R., 2003. Diabetes Technol. Ther. 5, 769–79.

Ferrante do Amaral, C.E., Wolf, B., 2008. Med. Eng. Phys. 30, 541–549.

Franklin, R.K., Johnson, M.D., Scott, K.A., Shim, J.H., Nam, H., Kipke, D.R., Brown, R.B., 2005. Proc. IEEE Sensors 2005, 1400–1403.

Frost, M.C., Meyerhoff, M.E., 2002. Curr. Opin. Chem. Biol. 6, 633–641.

Gifford, R., 2013. ChemPhysChem 14, 2032–2044.

Gosselin, B., 2011. Sensors 11, 4572-4597.

Groenendaal, W., Schmidt, K. a, von Basum, G., van Riel, N. a W., Hilbers, P. a J., 2008. Diabetes Technol. Ther. 10, 283–93.

Harrison, D.J., Turner, R.F.B., Baltes, H.P., 1988. Anal. Chem. 60, 2002–2007.

Heller, A., Feldman, B., 2010. Acc. Chem. Res. 43, 963–973.

Heller, A., Feldman, B., 2008. Chem. Rev. 108, 2482–2505.

Hilgers, M.E., Racchini, J.R., Hoegh, T.B., 2001. Diabetes Technol. Ther. 3, 81–90.

Hovorka, R., 2006. Diabet. Med. 23, 1–12.

Hwang, K., Kim, H., Kim, D.J., 2016. Microsurgery 36, 54–8.

Juodkazyte, J., ??ebeka, B., Valsiunas, I., Juodkazis, K., 2005. Electroanalysis 17, 947–952.

Koudelka, M., Gernet, S., Rooij, N.F.D.E., 1989. Sensors and Actuators 18, 157–165.

Le Floch, J.P., Bauduceau, B., Levy, M., Mosnier-Pudar, H., Sachon, C., Kakou, B., 2008. Diabetes Care 31(10), e73.

Li, C., Ahn, C.H., Shutter, L.A., Narayan, R.K., 2009. Biosens. Bioelectron. 25, 173–178.

Li, C.M., Dong, H., Cao, X., Luong, J.H.T., Zhang, X., 2007. Current Med. Chem. 14(8), 937-951.

Liu, Y., Wang, L., Liu, J., Di, Y., 2013. J. Therm. Biol. 38, 440–448.

Marunaka, Y., 2015. World J. Diabetes 6, 125–35.

Marzouk, S.A.M., Ufer, S., Buck, R.P., Johnson, T.A., Dunlap, L.A., Cascio, W.E., 1998. Anal. Chem. 70, 5054–5061.

Mukerjee, E. V., Collins, S.D., Isseroff, R.R., Smith, R.L., 2004. Sensors Actuators, A Phys. 114, 267–275.

Pang, C., Lee, C., Suh, K.Y., 2013. J. Appl. Polym. Sci. 130, 1429-1441.

Park, S., Boo, H., Chung, T.D., 2006. Anal. Chim. Acta 556, 46–57.

Park, S.I., Jun, S.B., Park, S., Kim, H.C., Kim, S.J., 2003. IEEE Sens. J. 3, 267–273.

Prausnitz, M.R., 2004. Adv. Drug Deliv. Rev. 56, 581–7.

Receveur, R.A.M., Lindemans, F.W., De Rooij, N.F., 2007. J. Micromech. Microeng. 17, R50-R80.

Shivashankar, M., Vinodini, V.R., Mishra, P., Uma, K., 2014. Int. J. Pharm. Pharm. Sci. 6(2), 1-5.

Suzuki, H., Hiratsuka, A., Sasaki, S., Karube, I., 1998. Sensors Actuators B Chem. 46, 104–113.

Toghill, K.E., Compton, R.G., 2010. Int. J. Electrochem. Sci. 5, 1246–1301.

Tolosa, V.M., Wassum, K.M., Maidment, N.T., Monbouquette, H.G., 2013. Biosens. Bioelectron. 42, 256–260.

Turner, R.F.B., Harrison, D.J., Rajotte, R. V., Baltes, H.P., 1990. Sensors Actuators B. Chem. 1, 561–564.

Turner, R.F.B., Harrison, D.J., Rojotte, R. V., 1991. Biomaterials 12, 361–368.

Vaddiraju, S., Burgess, D.J., Tomazos, I., Jain, F.C., Papadimitrakopoulos, F., 2010a. J. Diabetes Sci. Technol. 4, 1540–62.

Vaddiraju, S., Legassey, A., Wang, Y., Qiang, L., Burgess, D.J., Jain, F., Papadimitrakopoulos, F., 2011. J. Diabetes Sci. Technol. 5, 1044–51.

Vaddiraju, S., Tomazos, I., Burgess, D.J., Jain, F.C., Papadimitrakopoulos, F., 2010b. Biosens. Bioelectron. 25(7), 1553-1565.

Vashist, S.K., 2012. Anal. Chim. Acta 750, 16–27.

Vashist, S.K., Zheng, D., Al-Rubeaan, K., Luong, J.H.T., Sheu, F.S., 2011. Anal. Chim. Acta 703, 124–136.

Waleed Shinwari, M., Zhitomirsky, D., Deen, I.A., Selvaganapathy, P.R., Jamal Deen, M., Landheer, D., 2010. Sensors 10, 1679–1715.

Wang, J., 2008. Electrochem. Sensors, Biosens. their Biomed. Appl. 57–69.

Wang, P.M., Cornwell, M., Prausnitz, M.R., 2005. Diabetes Technol. Ther. 7, 131–41.

Wang, T., Cook, C.C., Serban, S., Ali, T., Drago, G., Derby, B., 2012. Arch. Condens. Matter 1–21.

Weltin, A., Enderle, B., Kieninger, J., Urban, G.A., 2014a. IEEE Sens. J. 14, 3345–3351.

Weltin, A., Kieninger, J., Enderle, B., Gellner, A.K., Fritsch, B., Urban, G.A., 2014b. Biosens. Bioelectron. 61, 192–199.

Yang, H., Chung, T.D., Kim, Y.T., Choi, C.A., Jun, C.H., Kim, H.C., 2002. Biosens. Bioelectron. 17, 251–259.

Yang, H., Kang, S.K., Choi, C.A., Kim, H., Shin, D.-H., Kim, Y.S., Kim, Y.T., 2004. Lab Chip 4, 42–46.

Yao, S., Wang, M., Madou, M., 2001. J. Electrochem. Soc. 148, H29.

Yu, L., Kim, B.J., Meng, E., 2014. Sensors 14, 20620–20644.

Figure/Table captions

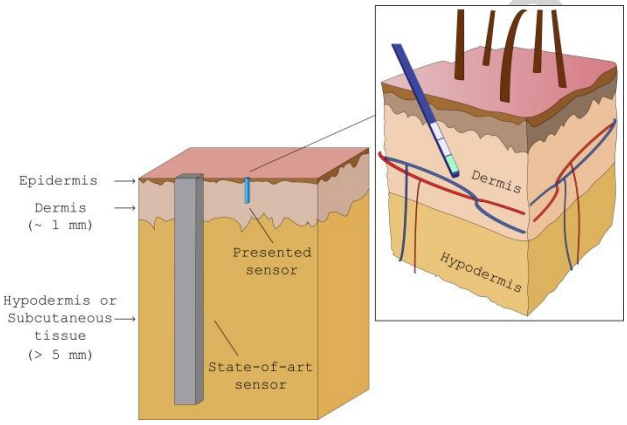

Fig. 1. In-scale cross-sectional drawing of the skin layers, depicting the possible use of a sensor with the presented miniaturized sensing area inserted in the dermal space, compared to the sensing portion of a state-of-the-art sensor (i.e. Abbott Freestyle™ Libre) having a much deeper penetration depth, operating in the subcutaneous tissue (or hypodermis). Inset: representation of the possible use of the device, with the active area of the three-electrode sensor inserted in the dermal space.

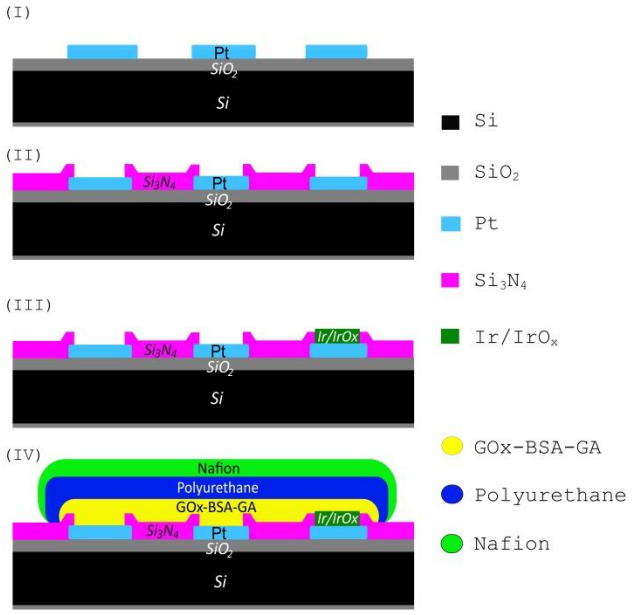

Fig. 2. Cross-sectional representation of the microfabrication steps, consisting in (I) platinum deposition, (II) passivation and electrode site opening, (III) iridium deposition and oxidation on the Q-RE site, and (IV) drop casting of the polymeric membranes. Diagrams are not to scale.

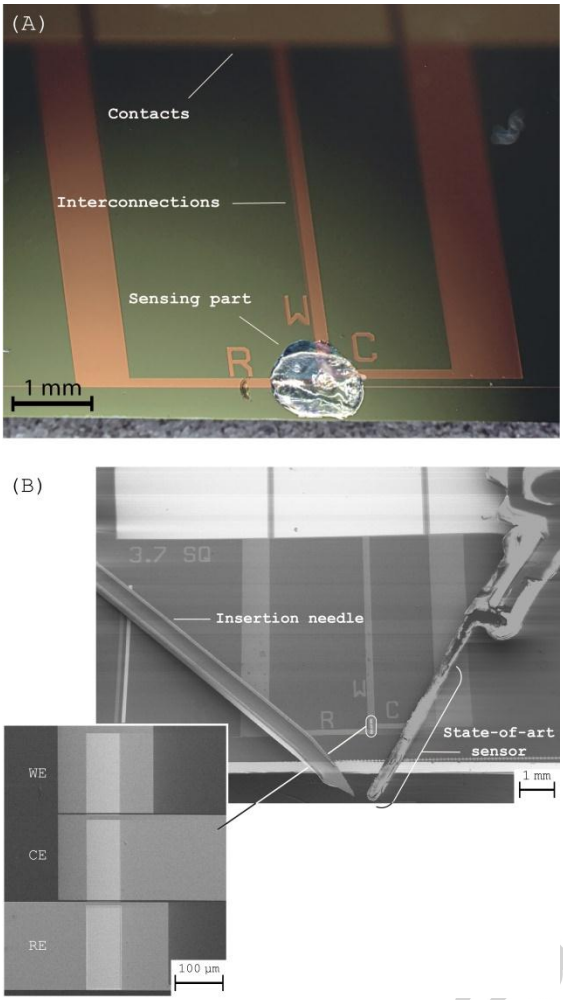

Fig. 3. (A) Optical top-view picture of the complete chip, with contacts on the top part, and active area, functionalized with the three polymeric membranes, in the lower part, as used for the characterization. (B) SEM picture of a bare chip sensing area, in the middle, compared to Abbott's Freestyle™ Libre sensor, on the right, and its insertion needle, on the left. Inset: SEM micrograph of the three microelectrodes before the deposition of the membranes, where WE and CE are made of platinum and the RE is covered with electrochemically oxidized iridium.

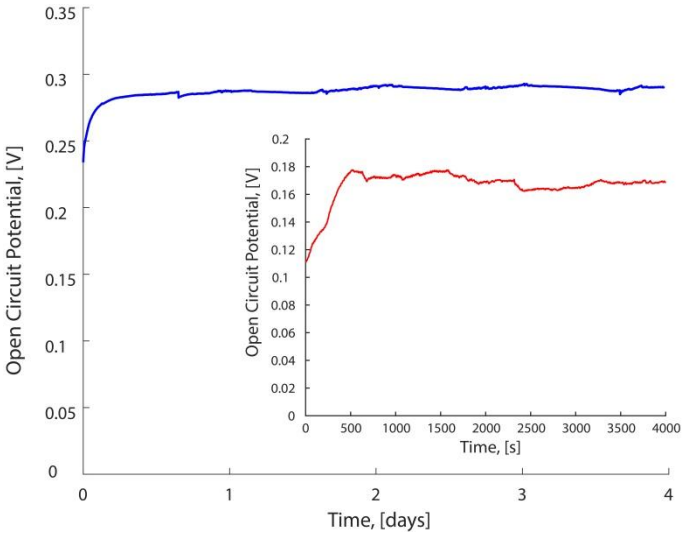

Fig. 4. Measurement of the open circuit potential of an oxidized iridium reference electrode (total geometrical area 0.012 mm^2) in a standard oxygen-containing PBS solution at 26 °C, over a four-day period. Inset: OCP measurement of another integrated iridium oxide Q-RE immediately after CV, in a deaerated PBS solution, showing a different absolute OCP value.

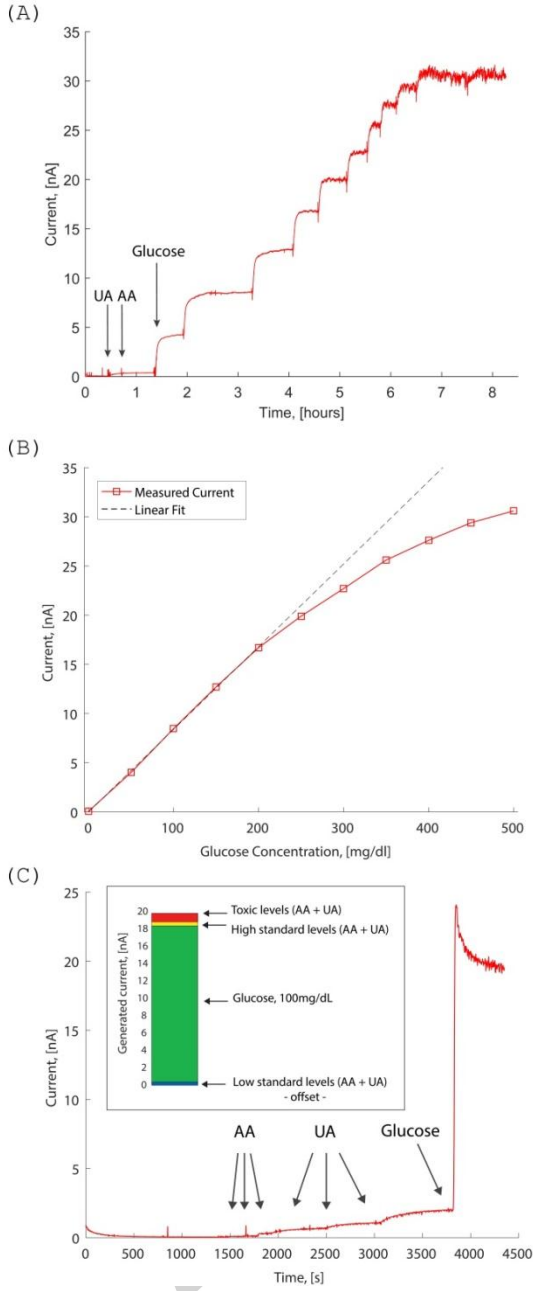

Fig. 5. (A) Chrono-amperometric measurement in PBS at increasing glucose concentrations, +50 mg/dL per step, and demonstration of selectivity towards possible interfering substances, namely UA and AA, using the described microsensor and the on-chip integrated IrOx Q-RE, over an eight-hour time frame. (B) Measured current as a function of the glucose concentration, from measurement A, and a linear fit of the curve. The linear fit follows the equation y = 0.084 [nA·mg^{-1}·dl] ·x + 0.074 [nA], having a linear correlation coefficient of 0.999 with the measurement data. A linear fit on the entire range can be instead expressed as y = 0.624 [nA·mg^{-1}·dl] ·x + 2.369 [nA], having a linear correlation coefficient of 0.986 with the measurement data. A bias of +0.5 V with respect to the embedded IrOx Q-RE was applied during measurements. (C) Chrono-amperometric characterization of the selectivity of the sensor, biased at +0.5 V with respect to the embedded IrOx Q-RE, at 34 °C in PBS solution. Aliquots at three increasing concentrations (low, high, and toxic) of AA and secondly UA have been added to the stirred solution, before adding glucose at a concentration of 100 mg/dL. Inset: graphical representation of the contribution of the different substances to the overall current, in which the current generated by low physiological levels of interferents can be considered as a minimum offset.

Highlights

- The smallest fully integrated planar glucose sensor area up-to-date is reported
- Microfabricated devices based on enzymatic electrochemical glucose sensing are shown
- A dynamic, linear and selective amperometric sensor has been characterized in-vitro
- A miniaturization sufficient to perform CGM in the dermis can be achieved
- Iridium oxide reference electrodes provide stability under physiological conditions